



Contents lists available at ScienceDirect

Tetrahedron Letters

journal homepage: [www.elsevier.com/locate/tetlet](http://www.elsevier.com/locate/tetlet)

## A chloroacetate based ratiometric fluorescent probe for cysteine detection in biosystems

Zhengkun Liu<sup>a,1</sup>, Qianqian Wang<sup>a,1</sup>, Hao Wang<sup>a</sup>, Wenting Su<sup>a</sup>, Shouliang Dong<sup>a,b,\*</sup>

<sup>a</sup> Institute of Biochemistry and Molecular Biology, School of Life Sciences, Lanzhou University, 222 Tianshui South Road, Lanzhou 730000, China

<sup>b</sup> Key Laboratory of Preclinical Study for New Drugs of Gansu Province, Lanzhou University, 222 Tianshui South Road, Lanzhou 730000, China

### ARTICLE INFO

#### Article history:

Received 31 July 2019

Revised 25 September 2019

Accepted 26 September 2019

Available online xxxxx

#### Keywords:

Chloroacetyl group

Fluorescent probe

Cysteine

Ratiometric

### ABSTRACT

The specific detection of cysteine (Cys) over homocysteine (Hcy), glutathione (GSH) and other amino acids is of great significance for studying its biological functions as well as for the diagnosis of related diseases. Chloroacetyl group was often used as a reaction site for cysteine fluorescent probes for its sensitivity and selectivity. However, high background fluorescence and low stability are common problems encountered by such probes. Here, four chloroacetyl group based fluorescent probes (**C1**, **C2**, **C3**, and **H4**) was synthesized for a comparative study. We found that the inefficient quenching ability of chloroacetyl group turned into an advantage when connected with a ratiometric fluorophore. With the modification of chloroacetyl group, probe **H4** displayed excellent ratiometric property and great selectivity for Cys, the stability was also improved. Additionally, the probe was successfully applied for quantitative detection of Cys in fetal bovine serum and real-time imaging in living HeLa cells with low toxicity.

© 2019 Elsevier Ltd. All rights reserved.

### Introduction

Biological thiols, such as cysteine (Cys), homocysteine (Hcy), and glutathione (GSH) are widely distributed and play key roles in the biological systems. In spite of their similar structures, biothiols have different biological functions. In mammalian cells, GSH is the most abundant intracellular non-protein thiol and plays a key role in the control of oxidative stress in redox homeostasis [1]. Mitochondrial GSH pool is a critical antioxidant reservoir within cells and associated with many mitochondria functions, such as signal transduction, and gene regulation [2]. The fluctuation of the levels of GSH is very important and has been linked to some diseases and dysfunction of mitochondrial [3,4]. Hcy is also one of the important biothiols and has gradually attracted widespread attention as a biomarker [5]. Clinical trial results have shown that high concentrations of Hcy in serum or plasma (mild: 15–30  $\mu\text{M}$ , moderate: 30–100  $\mu\text{M}$ , severe:  $\geq 100 \mu\text{M}$ ) are predictors of cardiovascular disease and independent risk factors. Elevated plasma homocysteine levels were found in Alzheimer's disease [6], Parkinson's disease [7,8], cancer [9–13], diabetes [14–16]. HIV-infected patients found a decrease in plasma homocysteine concentration [17]. Cys as a semi-essential amino acid and biothiol, is a very

important functional and structural moiety of various peptides or proteins. The deficiency of Cys would cause many symptoms like retarded growth in children, hair depigmentation, lethargy, liver damage, muscle and fat loss, skin lesions and weakness [18–21]. Furthermore, chronic accumulation of free Cys is related to neuro-pathic poisoning [22]. The role of Cys in various cancer is also important yet not completely clear [23,24]. Therefore, the specific detection of Cys is very important for studying its biological functions and for the diagnosis of related diseases.

Among various detection methods, fluorescent probes have emerged as the most common imaging strategy due to its simplicity, high sensitivity and non-destructive advantages [25]. In the past ten years, a large number of fluorescent probes for Cys detection have been developed based on different mechanisms [25,26]. Many response groups such as aldehyde group [27], acrylate [28], maleimide [29], 7-nitrobenzofurazan (NBD) [30] and various metal ions [31,32] were used to design probes for Cys. Chloroacetyl group was also employed for its great selectivity (Scheme 1). But compare to widely used acrylate, the same nucleophilic addition-cyclization type reaction group, the application of chloroacetyl group for Cys detection was relatively fewer. This may be caused by some disadvantages of chloroacetyl group, such as inefficient quenching ability which caused high background fluorescence, low stability and relatively slow reactivity [33–37]. To solve these problems, four chloroacetyl group based probes, **C1**, **C2**, **C3**, and **H4**, with different connecting structures and fluorophores were

\* Corresponding author.

E-mail address: [dongsl@lzu.edu.cn](mailto:dongsl@lzu.edu.cn) (S. Dong).

<sup>1</sup> These authors contributed equally to this work.



**Scheme 1.** Proposed response mechanism of chloroacetate-based probes to Cys.

designed and synthesised. The stability, reactivity and spectral properties of the four probes were thoroughly investigated. We found that the inefficient quenching ability of chloroacetyl group turned into an advantage when connected with a ratiometric fluorophore (**H4**) and with the addition of cetyltrimethylammonium bromide (CTAB), the stability and reactivity of **H4** were greatly improved. Additionally, probe **H4** was successfully applied for detecting and real-time imaging of Cys in fetal bovine serum and living HeLa cells with low toxicity.

## Results and discussion

As shown in Fig. 1, **C1** was constructed by a directly connection of chloroacetyl group with coumarin, while **C2** and **C3** were connected by 2-(hydroxymethyl)benzoic acid (HMBA) or 2-(2-hydroxyethyl)benzoic acid (HEBA) group for better quenching effect. The detailed information of synthesis for **C1**, **C2**, and **C3** was shown in ESI, the intermediates and final products were confirmed by  $^1\text{H}$  NMR,  $^{13}\text{C}$  NMR and mass spectrometry. Proposed response mechanisms of **C1**, **C2**, and **C3** for Cys detection were shown in Scheme S1. For **C2** and **C3**, after the addition-cyclization release of chloroacetyl group, the HMBA and HEBA group both can undergo another cascaded intramolecular cyclization reaction to generate the highly fluorescent coumarin. These groups were initially designed for the protecting of carbohydrates [38,39] and

HMBA and HEBA displayed different reactivity and stability when deprotection [39]. So, we employed both two groups for **C2** and **C3** design to achieve the completely quenching effect. With probes **C1**, **C2**, and **C3** in hand, we first investigated the quenching ability of chloroacetyl group (**C1**) and the new designed mask groups of **C2** and **C3**. As depicted in Fig. 2A, the high background fluorescence was observed in **C1** probably due to the inefficient quenching ability of chloroacetyl group mentioned above. Comparatively only weak background fluorescence was detected in **C2** and **C3**, this result indicated that connection with HMBA and HEBA greatly improved the quenching ability of chloroacetyl group. The improved quench effects may be caused by electron-withdrawing effect of ester bond [40] and the reduced rigidity of probes structure [41]. **C2** and **C3** also showed great selectivity for Cys over Hcy and GSH (Fig. 2B, 2C). We then further studied the kinetic properties of **C2** and **C3** upon reaction with three biothiols, unfortunately, we found that the stabilities of **C2** and **C3** were greatly influenced by temperature and polar solvents. In the biocompatible condition of 37 °C and 1% DMSO/PBS (V/V), **C2** and **C3** were completely hydrolyzed within 2 h which perhaps caused by two unstable ester bonds. So **C1**, **C2** and **C3** were not suitable for biological detection.

We further designed and synthesized **H4** through a directly linking between chloroacetyl group and 2-(2'-hydroxy-3'-methoxyphenyl)benzothiazole (HMBT), Scheme 2. HMBT is a widely used fluorophore for its small size, good photostability and relative biological compatibility [42]. Besides, HMBT can undergo an excited-state intramolecular photon transfer (ESIPT) process upon photoexcitation, resulting in dual emission bands which originate from its enol and keto tautomeric forms [43]. The detailed information of synthesis for **H4**, characteristic spectrums of the intermediates and final products can be seen in ESI. The absorption and fluorescence emission spectra of **H4** in the absence and presence of cysteine were shown in Fig. S1, as also the HMBT. In addition, the absolute quantum yield of **H4** in 320–420 nm were measured to be 0.49%. After addition of cysteine the emission redshifted to 450–600 nm and the absolute quantum yield was 0.48% compared to 0.61% of HMBT. **H4** displayed strong fluorescence at 372 nm which was in accordance with the emission band from enol forms

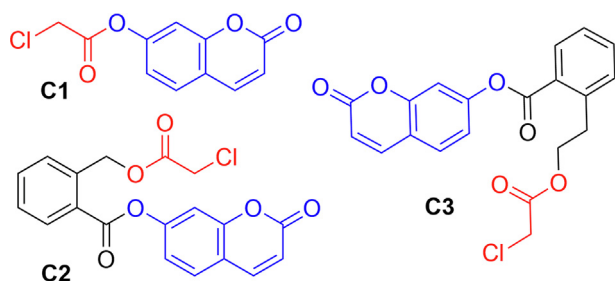


**Fig. 1.** The structure of probes **C1**, **C2**, and **C3**.

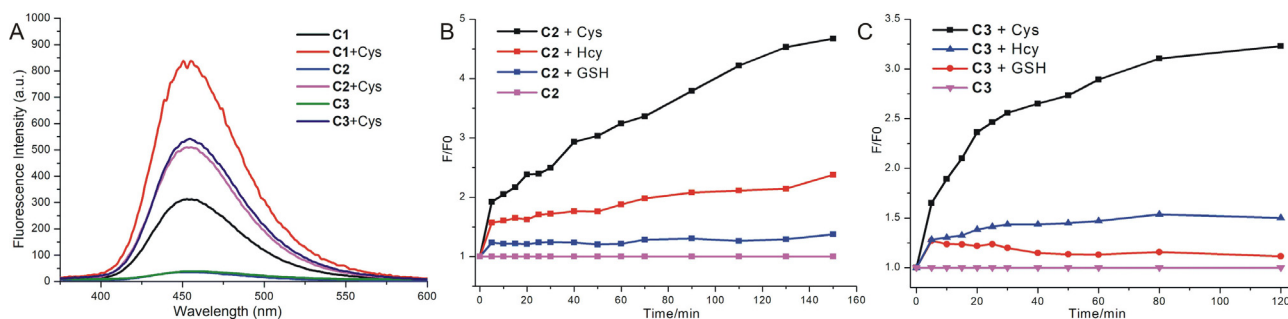
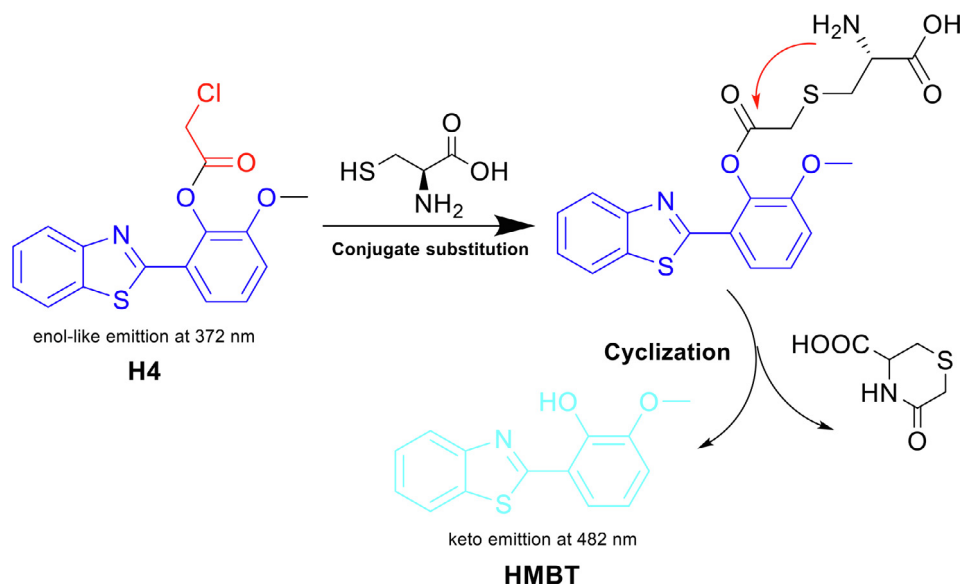


**Fig. 2.** (A) Fluorescence intensity changes of the probes **C1**, **C2**, and **C3** (all 10  $\mu\text{M}$ ) before and after treatment with 100  $\mu\text{M}$  Cys for 2 h; (B, C) Time-dependent fluorescence intensity ratios  $F/F_0$  of 10  $\mu\text{M}$  probes **C2** and **C3** after addition of Cys, Hcy and GSH 100  $\mu\text{M}$  respectively. All experiments carried in 50% ACN/PBS (V/V) buffer (50 mM, pH = 7.4) at 20 °C,  $\lambda_{\text{ex}} = 327$  nm,  $\lambda_{\text{em}} = 454$  nm, slits (10, 10).



**Scheme 2.** The structure of probe **H4**, **HMBT** and proposed response mechanism of **H4** to Cys.

of HMBT. This phenomenon was different with many other HMBT based probes, because the enol-like emission was usually quenched and only showed slightly changes after reacted with analytes [44–46]. Thus the inefficient quenching ability of chloroa-

cetyl group turned into an advantage when connected with HMBT. As expected, after treatment with Cys, the enol-like emission of **H4** declined and new emission at 482 nm appeared (Fig. 3A). The proposed response mechanism was also confirmed by mass and the

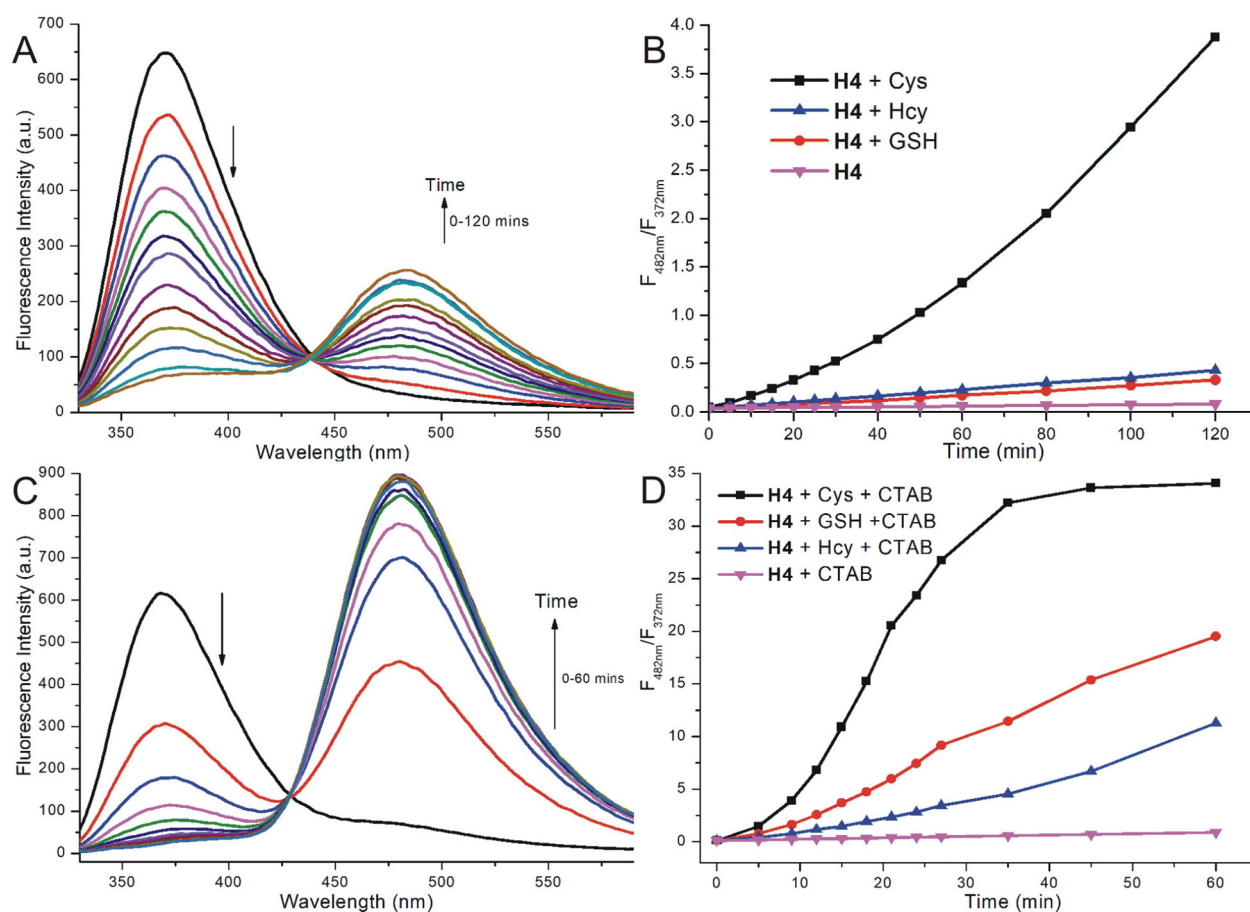


**Fig. 3.** (A, C) Time-dependent fluorescence intensity of 10  $\mu\text{M}$  **H4** upon addition of 500  $\mu\text{M}$  Cys; (B, D) Time-dependent fluorescence intensity ratios at  $F_{482\text{nm}}/F_{372\text{nm}}$  of 10  $\mu\text{M}$  probes **H4** after addition of Cys, Hcy and GSH, 500  $\mu\text{M}$  respectively. All experiments in A and B were carried in 50% ACN/PBS (V/V) buffer (50 mM, pH = 7.4) at 37  $^{\circ}\text{C}$ . All experiments in C and D were carried in 1% ACN/PBS (V/V) buffer (50 mM, pH = 7.4) with addition of 1 mM CTAB at 37  $^{\circ}\text{C}$ .  $\lambda_{\text{ex}} = 310\text{ nm}$ ,  $\lambda_{\text{em}} = 372\text{ nm}$ , 482 nm, slits (10, 10).

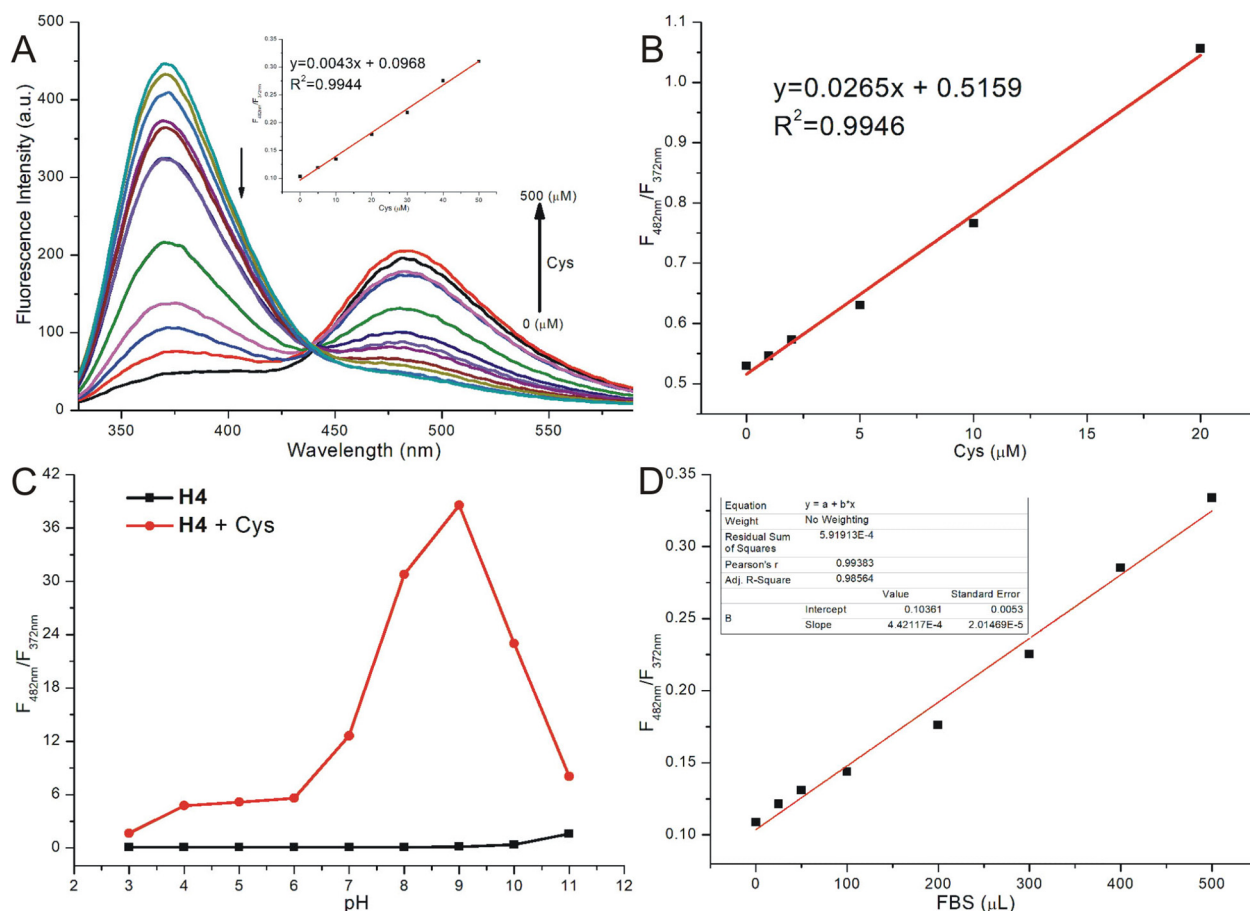


**Fig. 4.** (A) Concentration-dependent fluorescence spectra of **H4** (10  $\mu\text{M}$ ) upon addition of Cys (0–500  $\mu\text{M}$ ) and the linear relationship between the fluorescence intensity ratios at  $F_{482\text{nm}}/F_{372\text{nm}}$  and Cys (0–50  $\mu\text{M}$ ); (B) Linear relationship between the fluorescence intensity ratios at  $F_{482\text{nm}}/F_{372\text{nm}}$  and concentrations of Cys (0–20  $\mu\text{M}$ ) in 1% ACN/PBS (V/V) buffer (50 mM, pH = 7.4) with 1 mM CTAB at 37  $^{\circ}\text{C}$ ; (C) Fluorescence intensity ratios ( $F_{482\text{nm}}/F_{372\text{nm}}$ ) changes of the probe **H4** (10  $\mu\text{M}$ ) at different pH values in the absence or presence of Cys; (D) Linear relationship between the fluorescence intensity ratios at  $F_{482\text{nm}}/F_{372\text{nm}}$  of **H4** (10  $\mu\text{M}$ ) and FBS (0–500  $\mu\text{L}$ ). A, C and D all in 50% ACN/PBS (V/V) buffer (50 mM, pH = 7.4) at 37  $^{\circ}\text{C}$ ,  $\lambda_{\text{ex}} = 310\text{ nm}$ ,  $\lambda_{\text{em}} = 372\text{ nm}$ , 482 nm, slits (10, 10).

**Table 1**  
Determination of Cys in fetal bovine serum sample.<sup>a</sup>

Added Cys ( $\mu\text{M}$ )	Measured ( $\mu\text{M}$ )	Recovery (%)	RSD (n = 3, %)
0	21.02	–	2.7
5	26.11	100.36	3.1
10	31.79	102.48	3.3
20	37.76	92.04	3.7

<sup>a</sup> Conditions: 10  $\mu\text{M}$  **H4** in PBS buffer (50 mM, pH = 7.4, 50% ACN), incubated for 2 h,  $\lambda_{\text{ex}} = 310\text{ nm}$ ,  $\lambda_{\text{em}} = 372\text{ nm}/482\text{ nm}$ .

formation of thiomorpholinone was clearly showed in mass spectrum, calculated for 161.01, found  $m/z$  160.01  $[\text{M}-\text{H}]^-$  (Fig. S4).

Next we investigated the fluorescence sensing behavior of **H4** toward biothiols. Because of the low solubility of **H4** in PBS, we first chose 50% ACN/PBS as reaction solvent. As shown in Fig. 3B, although **H4** showed great selectivity to Cys over Hcy and GSH, the reaction rate was slow and it spent more than 2 h to complete the detection. The addition of surfactants such as CTAB were usually applied to improve the solubility and increase the kinetics of probes' reaction in aqueous solution [47,48]. With the addition of CTAB, **H4** can easily dissolved in 1% ACN/PBS and showed great stability, the keto emission of **H4** was also greatly enhanced (Fig. 3C). In this solvent condition, the reaction of **H4** with Cys was com-

pleted within 40 mins, the sensitivity of **H4** for Hcy was also slightly improved. But considering the relatively low content of Hcy in biosystem, the selectivity of **H4** for Cys would not be affected (Fig. 3D).

We then evaluated the sensitivity of **H4** for Cys. Concentration-dependent studies showed an excellent linearity between fluorescence intensity ratios at  $F_{482\text{nm}}/F_{372\text{nm}}$  and Cys (0–50  $\mu\text{M}$ ) in 50% ACN/PBS (V/V) buffer, with a calculated detection limit of 1.01  $\mu\text{M}$  (Fig. 4A). Besides, with the addition of CTAB in 1% ACN/PBS (V/V) buffer, the detection limit can as low as 0.4  $\mu\text{M}$  (Fig. 4B). These results showed that **H4** has enough sensitivity for Cys detection in biological systems. Furthermore, the excellent linearity equipped probe **H4** with the ability of quantitative detection of Cys.

The selectivity of **H4** for Cys over other amino acids was also evaluated. Significant fluorescent emission (Fig. S2) was induced only upon addition of Cys, indicating great selectivity of **H4** toward Cys. The pH effect of **H4** in the presence or absence of Cys was also investigated (Fig. 4C). The fluorescence spectra showed no significant change for the free probe over a wide pH range of 3.0–11.0, indicating that **H4** is very stable in a relatively wide pH range. On the other hand, upon treatment with Cys, there was a progressive fluorescence enhancement between pH 3.0 and 9.0, this may be partially caused by enhanced reactivity of **H4** under alkaline conditions, but stronger alkali seems to suppressed the

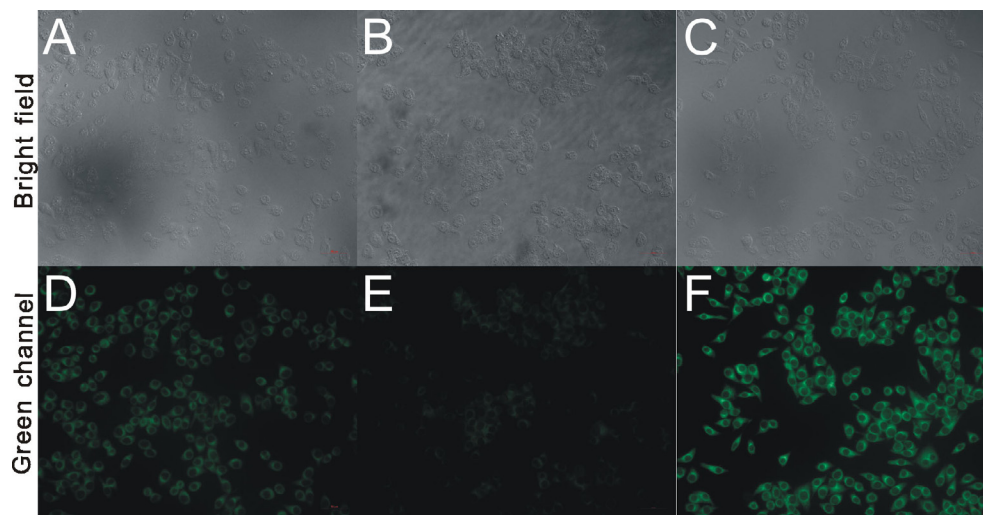


**Fig. 5.** Fluorescence images of HeLa cells. (A, D) Cells incubated with only **H4** (20  $\mu\text{M}$ ) for 10 min. (B, E) Cells incubated with NEM (200  $\mu\text{M}$ ) for 30 min before with **H4** (20  $\mu\text{M}$ ) for 10 min. (C, F) Cells incubated first with NEM (200  $\mu\text{M}$ ) for 30 min, then Cys (200  $\mu\text{M}$ ) for 30 min and finally **H4** (20  $\mu\text{M}$ ) for another 10 min. 37  $^{\circ}\text{C}$ , green channel: Ex = 426–446 nm, Em = 460–500 nm. (For interpretation of the references to colour in this figure legend, the reader is referred to the web version of this article.)

keto-emission of **H4** [49]. These results indicated that **H4** could serve as a satisfactory Cys sensing probe under physiological pH conditions.

Before the applications of **H4** for Cys detection in biosystems, standard methyl thiazolyl tetrazolium (MTT) assay was carried out to evaluate its cytotoxicity. After incubation with **H4** for 24 h, no significant reduction in cell viability can be observed with the probe at concentrations of 5–20  $\mu\text{M}$  (Fig. S3), indicating low cytotoxicity of **H4**. Then the detection of Cys in diluted (5%) reduced fetal bovine serum (FBS) was carried out. A concentration-dependent fluorescence intensity ratio increase ( $F_{482\text{ nm}}/F_{372\text{ nm}}$ ) was observed with excellent linearity characteristics (Fig. 4D). By using the standard addition method, the amount of Cys in the FBS sample was determined to be 384.5  $\mu\text{M}$  with satisfactory recovery (Table 1). The results suggested that the **H4** can be applied to the quantitative detection of Cys in serum samples.

We next evaluated the capability of the probe **H4** for Cys imaging in HeLa cells. As exhibited in Fig. 5, when HeLa cells were incubated with **H4** (20  $\mu\text{M}$ ) for 10 min, a strong green fluorescence enhancement was observed implying the long-wavelength keto emission of **H4**. In contrast, when HeLa cells were pre-treated with 1 mM NEM (N-ethylmaleimide, a commonly used intracellular thiol scavenger) before treated with **H4** (20  $\mu\text{M}$ ), the fluorescence intensity was decreased, but a strong fluorescence was recovered when 200  $\mu\text{M}$  Cys was added after treated with NEM, confirming unambiguously that the fluorescence was induced by Cys. This result showed that **H4** can sense Cys in living cells.

## Conclusions

The application of chloroacetyl group for Cys detection was limited by its inefficient quenching ability, low stability and relatively slow reactivity. We rationally designed and synthesised four chloroacetyl group based probes, **C1**, **C2**, **C3**, and **H4**, with different connecting structure and fluorophores. We found that the inefficient quenching ability of chloroacetyl group turned into an advantage when connected with ratiometric fluorophore HMBT. **H4** displayed excellent ratiometric property and great selectivity for Cys, with the addition of CTAB, the stability and reactivity of **H4** were greatly improved. Additionally, probe **H4** was successfully applied for detecting and real time imaging of Cys in FBS and living HeLa cells with low toxicity. The short excitation wavelength of **H4** is a draw-

back for its application in living system imaging and a near-infrared ratiometric fluorophore is needed.

## Declaration of Competing Interest

The authors declare that they have no known competing financial interests or personal relationships that could have appeared to influence the work reported in this paper.

## Acknowledgements

The authors want to thank Mr. Feiyun Gao (School of Basic Medical Sciences, Lanzhou University) for the Mass spectra, Mr. Shunxi Li (Northwest Normal University, Gansu, China) for the NMR spectra, Core Facility of School of Life Sciences (Lanzhou University) for the imaging and the Central Laboratory (the First Hospital, Lanzhou University) for the cell experiments.

## Appendix A. Supplementary data

Supplementary data to this article can be found online at <https://doi.org/10.1016/j.tetlet.2019.151218>.

## References

- [1] M. Mari, A. Morales, A. Colell, C. Garcia-Ruiz, J.C. Fernandez-Checa, Mitochondrial glutathione, a key survival antioxidant, *Antioxid. Redox Signal.* 11 (2009) 2685–2700.
- [2] V. Ribas, C. Garcia-Ruiz, J.C. Fernandez-Checa, Glutathione and mitochondria, *Front. Pharmacol.* 5 (2014) 151.
- [3] Y.H. Han, S.Z. Kim, S.H. Kim, W.H. Park, Apoptosis in pyrogallol-treated Calu-6 cells is correlated with the changes of intracellular GSH levels rather than ROS levels, *Lung Cancer* 59 (2008) 301–314.
- [4] Y.H. Han, S.H. Kim, S.Z. Kim, W.H. Park, Apoptosis in arsenic trioxide-treated Calu-6 lung cells is correlated with the depletion of GSH levels rather than the changes of ROS levels, *J. Cell. Biochem.* 104 (2008) 862–878.
- [5] A.R. Folsom, Classical and novel biomarkers for cardiovascular risk prediction in the United States, *J. Epidemiol.* 23 (2013) 158–162.
- [6] K. Nilsson, L. Gustafson, B. Hultberg, Elevated plasma homocysteine level is not primarily related to Alzheimer's disease, *Dement. Geriatr. Cogn. Disord.* 34 (2012) 121–127.
- [7] M.C. Rodriguez-Oroz, P.M. Lage, J. Sanchez-Mut, I. Lamet, J. Pagonabarraga, J.B. Toledo, D. Garcia-Garcia, P. Clavero, L. Samaranch, C. Irurzun, Homocysteine and cognitive impairment in Parkinson's disease: a biochemical, neuroimaging, and genetic study, *Mov. Disord.* 24 (2009) 1437–1444.
- [8] S. Zoccollella, C. dell'Aquila, G. Abuzzese, A. Antonini, U. Bonuccelli, M. Canesi, S. Cristina, R. Marchese, C. Pacchetti, R. Zagaglia, Hyperhomocysteinemia in

- levodopa-treated patients with Parkinson's disease dementia, *Mov. Disord.* 24 (2009) 1028–1033.
- [9] M. Kędzierska, R. Głowacki, U. Czernek, K. Szydłowska-Pazera, P. Potemski, J. Piekarski, A. Jeziorski, B. Olas, Changes in plasma thiol levels induced by different phases of treatment in breast cancer; the role of commercial extract from black chokeberry, *Mol. Cell. Biochem.* 372 (2013) 47–55.
- [10] J.W. Miller, S.A. Beresford, M.L. Neuhouser, T.-Y.D. Cheng, X. Song, E.C. Brown, Y. Zheng, B. Rodriguez, R. Green, C.M. Ulrich, Homocysteine, cysteine, and risk of incident colorectal cancer in the Women's Health Initiative observational cohort, *Am. J. Clin. Nutr.* 97 (2013) 827–834.
- [11] N.S. Mohammad, R. Yedluri, P. Addepalli, S.R. Gottumukkala, R.R. Digumarti, V. K. Kutala, Aberrations in one-carbon metabolism induce oxidative DNA damage in sporadic breast cancer, *Mol. Cell. Biochem.* 349 (2011) 159–167.
- [12] S. Pathak, N. Bhatla, N. Singh, Cervical cancer pathogenesis is associated with one-carbon metabolism, *Mol. Cell. Biochem.* 369 (2012) 1–7.
- [13] S. Stabler, T. Koyama, Z. Zhao, M. Martinez-Ferrer, R.H. Allen, Z. Luka, L.V. Loukachevitch, P.E. Clark, C. Wagner, N.A. Bhowmick, Serum methionine metabolites are risk factors for metastatic prostate cancer progression, *PLoS ONE* 6 (2011) e22486.
- [14] M.Y. Al-Maskari, M.I. Waly, A. Ali, Y.S. Al-Shuaibi, A. Ouhit, Folate and vitamin B12 deficiency and hyperhomocysteinemia promote oxidative stress in adult type 2 diabetes, *Nutrition* 28 (2012) e23–e26.
- [15] M. Isokawa, T. Kanamori, T. Funatsu, M. Tsunoda, Analytical methods involving separation techniques for determination of low-molecular-weight biothiols in human plasma and blood, *J. Chromatogr. B* 964 (2014) 103–115.
- [16] C.-J. Tsai, C.-J. Hsieh, S.-C. Tung, M.-C. Kuo, F.-C. Shen, Acute blood glucose fluctuations can decrease blood glutathione and adiponectin levels in patients with type 2 diabetes, *Diabetes Res. Clin. Pract.* 98 (2012) 257–263.
- [17] I. Muneke, K. Takahiro, F. Takashi, T. Makoto, Analytical methods involving separation techniques for determination of low-molecular-weight biothiols in human plasma and blood, *J. Chromatogr. B* 964 (2014) 103–115.
- [18] J.H. Fox, D.S. Barber, B. Singh, B. Zucker, M.K. Swindell, F. Norflus, R. Buzescu, R. Chopra, R.J. Ferrante, A. Kazantsev, S.M. Hersch, Cystamine increases l-cysteine levels in Huntington's disease transgenic mouse brain and in a PC12 model of polyglutamine aggregation, *J. Neurochem.* 91 (2004) 413–422.
- [19] B.D. Paul, J.I. Sbdio, R. Xu, M.S. Vandiver, J.Y. Cha, A.M. Snowman, S.H. Snyder, Cystathionine  $\gamma$ -lyase deficiency mediates neurodegeneration in Huntington's disease, *Nature* 509 (2014) 96.
- [20] K.G. Reddie, K.S. Carroll, Expanding the functional diversity of proteins through cysteine oxidation, *Curr. Opin. Chem. Biol.* 12 (2008) 746–754.
- [21] Z.A. Wood, E. Schröder, J. Robin Harris, L.B. Poole, Structure, mechanism and regulation of peroxiredoxins, *Trends Biochem. Sci.* 28 (2003) 32–40.
- [22] V. Gazit, R. Ben-Abraham, R. Coleman, A. Weizman, Y. Katz, Cysteine-induced hypoglycemic brain damage: an alternative mechanism to excitotoxicity, *Amino Acids* 26 (2004) 163–168.
- [23] W. Dröge, A. Gross, V. Hack, R. Kinscherf, M. Schykowski, M. Bockstette, S. Mihm, D. Galter, Role of Cysteine and Glutathione in HIV Infection and Cancer Cachexia: Therapeutic Intervention with N-Acetylcysteine, in: H. Sies (Ed.), *Advances in Pharmacology*, Academic Press, 1996, pp. 581–600.
- [24] J.W. Miller, S.A. Beresford, M.L. Neuhouser, T.-Y.D. Cheng, X. Song, E.C. Brown, Y. Zheng, B. Rodriguez, R. Green, C.M. Ulrich, Homocysteine, cysteine, and risk of incident colorectal cancer in the Women's Health Initiative observational cohort, *Am. J. Clin. Nutr.* 97 (2013) 827–834.
- [25] X. Chen, Y. Zhou, X. Peng, J. Yoon, Fluorescent and colorimetric probes for detection of thiols, *Chem. Soc. Rev.* 39 (2010) 2120–2135.
- [26] F. Yan, X. Sun, F. Zu, Z. Bai, Y. Jiang, K. Fan, J. Wang, Fluorescent probes for detecting cysteine, *Method. Appl. Fluoresc.* 6 (2018) 042001.
- [27] Y. Li, A ratiometric fluorescent chemosensor for the detection of cysteine in aqueous solution at neutral pH, *Luminescence* 32 (2017) 1385–1390.
- [28] Y. Yu, J. Yang, X. Xu, Y. Jiang, B. Wang, A novel fluorescent probe for highly sensitive and selective detection of cysteine and its application in cell imaging, *Sens. Actuators, B* 251 (2017) 902–908.
- [29] Z. Chen, Q. Sun, Y. Yao, X. Fan, W. Zhang, J. Qian, Highly sensitive detection of cysteine over glutathione and homo-cysteine: New insight into the Michael addition of mercapto group to maleimide, *Biosens. Bioelectron.* 91 (2017) 553–559.
- [30] P. Wang, Y. Wang, N. Li, J. Huang, Q. Wang, Y. Gu, A novel DCM-NBD conjugate fluorescent probe for discrimination of Cys/Hcy from GSH and its bioimaging applications in living cells and animals, *Sens. Actuators, B* 245 (2017) 297–304.
- [31] G. Liao, C. Zheng, D. Xue, C. Fan, G. Liu, S. Pu, A diarylethene-based fluorescent chemosensor for the sequential recognition of Fe<sup>3+</sup> and cysteine, *RSC Adv.* 6 (2016) 34748–34753.
- [32] S. Das, Y. Sarkar, R. Majumder, S. Mukherjee, J. Bandyopadhyay, A. Ray, P.P. Parui, A unique cysteine selective water soluble fluorescent probe operable in multiple sensing cycles for the detection of biogenic cysteine in multicellular living species, *New J. Chem.* 41 (2017) 1488–1498.
- [33] Y. Yu, H. Xu, W. Zhang, B. Wang, Y. Jiang, A novel benzothiazole-based fluorescent probe for cysteine detection and its application on test paper and in living cells, *Talanta* 176 (2018) 151–155.
- [34] J. Hou, P. Cai, C. Wang, Y. Shen, A novel fluorescent probe with a large Stokes shift for cysteine based on dicyanoisophorone, *Tetrahedron Lett.* 59 (2018) 2581–2585.
- [35] J. Yang, Y. Yu, B. Wang, Y. Jiang, A sensitive fluorescent probe based on coumarin for detection of cysteine in living cells, *J. Photochem. Photobiol., A* 338 (2017) 178–182.
- [36] B. Zhu, Y. Zhao, Q. Zhou, B. Zhang, L. Liu, B. Du, X. Zhang, A chloroacetate-caged fluorescein chemodosimeter for imaging cysteine/homocysteine in living cells, *Eur. J. Org. Chem.* 2013 (2013) 888–893.
- [37] J. Wang, C. Zhou, W. Liu, J. Zhang, X. Zhu, X. Liu, Q. Wang, H. Zhang, A near-infrared fluorescent probe based on chloroacetate modified naphthofluorescein for selectively detecting cysteine/homocysteine and its application in living cells, *Photochem. Photobiol. Sci.* 15 (2016) 1393–1399.
- [38] T. Ziegler, G. Pantkowski, The 2-(chloroacetoxyethyl) benzoyl (CAMB) Group as a Novel Protecting Group for Carbohydrates, *Liebigs Ann. Chem.* 1994 (1994) 659–664.
- [39] T. Ziegler, G. Pantkowski, The 2-(2-chloroacetoxyethyl)benzoyl group – stable to hydrogenolysis and cleavable beside other acyl groups, *Tetrahedron Lett.* 36 (1995) 5727–5730.
- [40] T. Wang, Y. Chai, S. Chen, G. Yang, C. Lu, J. Nie, C. Ma, Z. Chen, Q. Sun, Y. Zhang, J. Ren, F. Wang, W.-H. Zhu, Near-infrared fluorescent probe for imaging nitroxyl in living cells and zebrafish model, *Dyes Pigm.* 166 (2019) 260–265.
- [41] T. Saha, D. Kand, P. Talukdar, Performance comparison of two cascade reaction models in fluorescence off-on detection of hydrogen sulfide, *RSC Adv.* 5 (2015) 1438–1446.
- [42] A.C. Sedgwick, L. Wu, H.-H. Han, S.D. Bull, X.-P. He, T.D. James, J.L. Sessler, B.Z. Tang, H. Tian, J. Yoon, Excited-state intramolecular proton-transfer (ESIPT) based fluorescence sensors and imaging agents, *Chem. Soc. Rev.* 47 (2018) 8842–8880.
- [43] X. Yang, Y. Guo, R.M. Strongin, Conjugate addition/cyclization sequence enables selective and simultaneous fluorescence detection of cysteine and homocysteine, *Angew. Chem. Int. Ed.* 50 (2011) 10690–10693.
- [44] Z. Huang, S. Ding, D. Yu, F. Huang, G. Feng, Aldehyde group assisted thiolysis of dinitrophenyl ether: a new promising approach for efficient hydrogen sulfide probes, *Chem. Commun.* 50 (2014) 9185–9187.
- [45] T. Gao, P. Xu, M. Liu, A. Bi, P. Hu, B. Ye, W. Wang, W. Zeng, A water-soluble ESIPT fluorescent probe with high quantum yield and red emission for ratiometric detection of inorganic and organic palladium, *Chem.-Asian J.* 10 (2015) 1142–1145.
- [46] L. Tang, M. Tian, H. Chen, X. Yan, K. Zhong, Y. Bian, An ESIPT-based mitochondria-targeted ratiometric and NIR-emitting fluorescent probe for hydrogen peroxide and its bioimaging in living cells, *Dyes Pigm.* 158 (2018) 482–489.
- [47] T. Haiyu, Q. Junhong, S. Qian, J. Chenjia, Z. Runsheng, Z. Weibing, A coumarin-based fluorescent probe for differential identification of sulfide and sulfite in CTAB micelle solution, *Analyst* 139 (2014) 3373–3377.
- [48] L. Tianbao, L. Jie, L. Zhen, L. Lin, S. Yuning, Z. Hailiang, Q. Yong, Imaging of living cells and zebrafish in vivo using a ratiometric fluorescent probe for hydrogen sulfide, *Analyst* 140 (2015) 7165.
- [49] H. Liu, X. Wang, Y. Xiang, A. Tong, Fluorescence turn-on detection of cysteine over homocysteine and glutathione based on "ESIPT" and "AIE", *Anal. Methods* 7 (2015) 5028–5033.